Hindawi
Advances in Civil Engineering
Volume 2022, Article ID 7734078, 12 pages
https://doi.org/10.1155/2022/7734078

Research Article

Deformation and Fracture Characteristics of Coal Gangue Interbedded Samples under Loading and Unloading Conditions

Jisheng Xue and Tielin Zhao

China Coal Research Institute, Beijing 100013, China

Correspondence should be addressed to Jisheng Xue; xuejisheng@tdkcsj.com

Received 20 February 2022; Revised 10 June 2022; Accepted 13 June 2022; Published 14 July 2022

Academic Editor: Zhijun Xu

The dynamic sedation of the coal mine production is alternate or superimposed in coal rocks, which causes crack unevenness due to the presence of jacquards, causing unregistered coal blocks. By observing the deformation and fracture characteristics of coal-rock interbedding specimens with different gangue ratio under different stress paths, this paper studies the fracture instability mechanism and fracture characteristics of coal-rock interbedding, analyzes the progressive failure process and fracture opening model of coal-rock interbedding, and uses GDEM software to simulate the triaxial loading and unloading failure characteristics of coal-rock samples. The results show that the ratio of gangue inclusion has a significant effect on the structural strength of coal rock interbedding; with the unloading, the coal rock interbedding of the top coal body will be damaged and destroyed to varying degrees and asynchronously, the coal rock interbedding of the top coal body will present various forms of failure characteristics according to the changes of horizontal stress gradient in the vertical direction; the progressive failure process of coal rock interbedding under loading and unloading conditions can be divided into three stages. As the jigs are raised, the crack nonstable expansion stress of the composite coal body sample is gradually increased; and the rising ratio of the jacket X is not complete. The striped conjugated shear failure characteristics are more obvious; the different combined coal gangue tester shows microcrack near the peripheral loading boundary, and as the loading axis pressure increases, the fracture distribution range and density are increased; the rock layer is present. The tensile fracture is destroyed, and the coal seam exhibits shear destruction of intensive cracks; different test pieces produce significant tensile destruction on one side of the unloaded boundary; the greater the loaded axial pressure of the specimen, the greater the damage degree of the specimen after unloading; the damage degree of two coal and one rock specimens is the largest, the damage degree of one coal and one rock specimens is in the middle, and the damage degree of one coal and two rock specimens is the smallest.

1. Introduction

Due to the complexity of coal-forming environment, gangue is often associated with coal roof. With the increase of coal roof thickness, coal-gangue interbed is the most common in extra-thick coal roof [1, 2]. A large number of on-field experience and laboratory studies show that the gangue layer in coal roof can cause poor caving performance and low recovery rate of top coal during fully mechanized caving mining of extra-thick coal roof. The reason is that the storage of gangue layer causes uneven development of fracture damage in top coal body, which is the main reason for aggravating coal deformation [3–8]. In the mining process, the disturbance of dynamic and static load alternates or superposes on the gangue coal roof, resulting in the excessive deformation bearing capacity of the coal body on the top of coal-gangue interbed, which leads to the failure instability or shear slip of the composite coal-gangue mass, resulting in irreversible large deformation, and the caving lumpiness of the top coal increases. The failure process of composite roof coal body is similar to the loading and unloading process. In the process of working face advancing, the coal body in the coal roof of coal-gangue interlayer experiences the failure through loading and unloading under the influence of the front abutment pressure [9–13]. The study shows that the controlling factors affecting the instability of coal mass are mainly the direction of stress, the rate of stress change, the physical and mechanical strength, and the friction properties of coal mass [14, 15].

Research reports on the failure of coal-gangue interbed focus on the uniaxial failure characteristics of coal-gangue interbed under dynamic and static loads and pay more attention to the influence of coal-gangue interbed on roof caving and impact liability. Zhu et al. [16] used standard rock specimens of 50 mm to study the uniaxial compression failure characteristics of coal-gangue interbeds with different thicknesses and inclinations. When the combination angle is less than 45°, the main failure is split failure, and when the combination angle is greater than 45°, the failure is shear failure along the interface. Wu et al. [17] used physical similarity simulation experiment to analyze the stress distribution and evolution law of coal-gangue interbedded roof and found that the advance pressure generated by mining led to the failure of coal-gangue interbedded roof, roof separation, subsidence, and caving. Zhang et al. [18] explained the factors influencing the mechanics and failure characteristics of combined coal-gangue through uniaxial and triaxial compressive tests of coal-gangue specimens in different combination forms and proposed that the failure of combined coal-gangue under load is mainly tensile failure and shear failure of coal body, and the damage of coal body can induce the damage or failure of rock body to a certain extent. Nie et al. [19, 20] found through laboratory tests that the fracture characteristics of combined coal-gangue mass in the process of uniaxial compression are different from those of single coal-gangue mass, and the fracture is progressive and the main fracture mechanism is shear failure. Zhao et al. [21, 22] combined the two-body interaction theory to explain the elastic rebound and strain localization characteristics of the two-body interaction system and proposed that the combined coal-gangue specimens could reflect the basic mechanical phenomena in the process of rock burst. Huang and Liu [23] studied the dynamic failure characteristics of coal-gangue under different loading speeds through the uniaxial loading test of combined coal-gangue. Liu et al. [24–26] carried out the study on the influencing factors of the bursting liability of combined coal-gangue, studied the bursting liability of combined coal-gangue by comparing the characteristics of coal-gangue combination obtained from the test, and obtained the correlation between the bursting liability of combined coal and various physical and mechanical parameters. Xie et al. [27, 28] analyzed the difference between single and aggregate mechanical properties through uniaxial and triaxial compression tests of combined coal-gangue and established a biophysical model, providing a theoretical basis for the study of biophysical stability. The failure mechanism of coal-gangue interbed may be the failure caused by the change of uniaxial stress condition from uniaxial stress condition to uniaxial stress condition, and the failure forms of coal body under different stress paths are obviously different. In the process of coal mining, the negative impact on production is mainly caused by the unloading process of coal-gangue interbed after the pressure rises. It is of great significance to clarify the unloading failure mechanism of coal-gangue interbed. Unloading rate, triaxial stress, soft structural plane, and gangue ratio all have an impact on the failure characteristics of coal-gangue interbed.

Figure 1: Coal-gangue interbed specimens.

The structure of single coal-gangue surface and simple combination of structural plane deformation and instability of coal-gangue damage characteristics for more in-depth research and roof caving in thick coal roof mining help to effectively control impact ground pressure and roadway instability but with compound roof coal in coal-gangue under static loading, the failure mechanism of fracture characteristics of the research is not comprehensive enough. In particular, there are few research works on the failure and instability of coal-gangue interbedded top and the influence of gangue ratio on the failure. In this paper, the failure mechanism and failure characteristics of the coal-gangue specimens with different ratios of gangue were studied by observing the deformation and failure laws of the coal-gangue specimens with different ratios of gangue.

2. Test Method

2.1. Specimens. In this paper, 150 mm × 150 mm × 150 mm coal-gangue interbed specimens were selected, and all specimens were taken from the same intact unweathered coal-gangue blocks. The specimen was produced in Madaotou Coal Mine in Datong, Shanxi Province; the embedded depth is 350 m. Coal bodies with dense and uniform texture were selected and bonded with gangue after processing. Each end face of the specimen was polished in the rock specimen processing workshop, and the size error of each direction of the specimen was less than 0.1 mm. The angle error of each face measured by the square is less than 0.1°. Before the experiment, the specimens were stored for half a month and dried naturally for the experiment. As shown in Figure 1, three combinations are selected according to different coal roof proportions, which are divided into three conditions: two coals and one gangue, one rock and one coal, and two rocks and one gangue.

2.2. Test Equipment and Test Principle. The failure and instability of rock mass are the result that the microdamage in rock mass accumulates to produce the main fracture surface

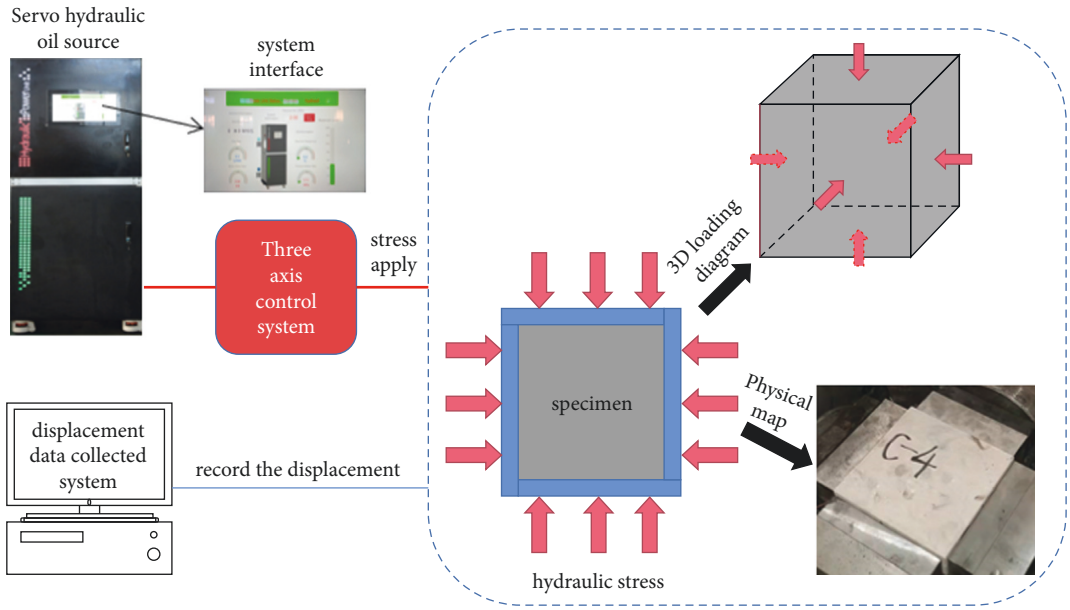

Figure 2: Principle of rock mechanics test system.

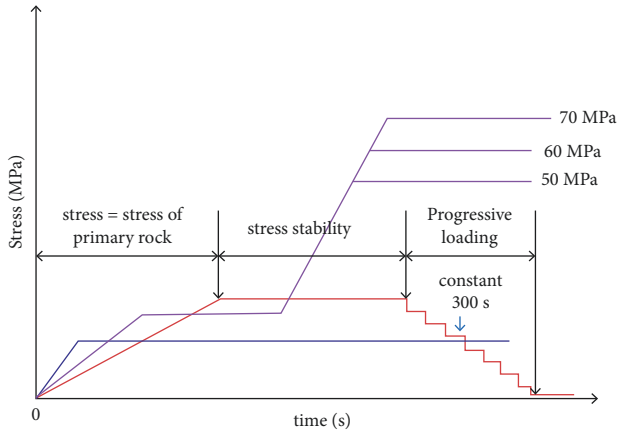

Figure 3: Stress loading and unloading test plan.

under the inducement of external force. The failure and instability of rock mass are a typical nonlinear failure. The study shows that the slight change of initial conditions in nonlinear system may lead to the great difference of the final failure form. For the research object of coal-gangue interbed, which is composed of a variety of rocks, there is a natural soft interface between coal body and rock stratum, and the thicknesses of gangue and coal-gangue interbed interface are bound to affect the deformation and failure characteristics of coal-gangue interbed specimens under the action of loading and unloading caused by mining, as well as the fracture structure generated within them.

In order to study the macroscopic and microscopic characteristics of deformation and fracture of coal-gangue interbedded specimens under loading and unloading conditions, the loading and unloading tests of coal-gangue interbedded specimens and CT scanning of fracture structures in rock mass were carried out by using true triaxial press and industrial microscopic CT imaging system, respectively. The principle of the test system is shown in Figure 2. The true triaxial rock press machine and CT scanning equipment used in this paper were provided by Central South University and Taiyuan University of Technology, respectively. The maximum load of the equipment is 2 000 kN, the loading rate is 10 N–10 kN/s, the accuracy is ±1%, the displacement measurement range is 0–200 mm, the measurement accuracy is <±0.5% FS, and the resolution of the minimum displacement is 0.001 mm.

2.3. Loading and Unloading Plans. The true triaxial loading mechanical test system was used to conduct mechanical tests on coal-gangue interbedded specimens to study the failure characteristics of coal-gangue under specific loading and unloading paths conforming to the advanced abutment pressure curve. The maximum principal stress in vertical bedding direction is the main factor causing the interbed in coal-gangue. According to the field measurement results, the axial pressures of 70 MPa, 60 MPa, and 50 MPa are taken, the maximum horizontal principal stress is 11.84 MPa, and the minimum horizontal principal stress is 6 MPa. The loading and unloading tests of coal-rock interbedded structure specimens under three kinds of combination conditions were carried out, respectively. According to the relevant test provisions of rock mechanics, the loading rate is 1 kN/s and the unloading rate is 0.2 kN/s. The loading plan is shown in Figure 3, y-axis refers to vertical stress (MPa). The vertical stress direction is the direction of the vertical specimen bedding, and the maximum horizontal principal stress direction is the unloading direction.

As shown in the table and figures, the most axial pressure of loading plan 1 is 70 MPa, the most axial pressure of loading plan 2 is 60 MPa, the most axial pressure of loading plan 3 is 50 MPa, and the specimen numbers and loading experiment plan are shown in Table 1.

Table 1: Specimens and the according load plan.

Specimen number	The type of specimens	Ratio of gangue (%)	Load plan
A3	One rock and one coal	50	Plan 2
A5	One rock and one coal	50	Plan 1
A6	One rock and one coal	50	Plan 3
B2	Two coals and one rock	33.3	Plan 2
B4	Two coals and one rock	33.3	Plan 1
B6	Two coals and one rock	33.3	Plan 3
C4	Two rocks and one coal	67.7	Plan 3
C5	Two rocks and one coal	67.7	Plan 2
C6	Two rocks and one coal	67.7	Plan 1

3. Deformation Characteristics of Specimens under Different Loading and Unloading Conditions

3.1. Failure Characteristics of Coal-Gangue Interbed Specimens. After the loading and unloading test, micro-CT was used to observe the crack morphology in the specimen. Figure 4 shows the micro-CT scanning results of the coal-gangue interbed specimen after loading and unloading. Among the 9 specimens, specimen C6 did not have integrity after loading and unloading and was not scanned. After analyzing the CT scanning results of each group of test pieces after loading and unloading test, the samples of coal rock combination with different gangue ratio have different failure characteristics, the sample has experienced the process of initial fracture compression, micro fracture development, interconnection, and finally the formation of through macro fractures, the failure mode is tension shear composite failure, the macrocracks of the specimen are obvious after failure.

Under the loading condition of plan 1, two rocks and one gangue specimen C6, one rock and one coal specimen A5, and two coals and one gangue specimen B4, all specimens were destroyed after unloading. Specimen C6 was destroyed after the experiment, and the specimen had no integrity after the experiment. The integrity of specimen A5 was damaged before the experiment, and there were obvious cracks and structural planes. It could be found that the cracks were mainly parallel to the direction of the minimum principal stress, and the fracture plane was x-shaped conjugate shear failure. The integrity of gangue was significantly stronger than that of coal. The deformation of specimen B4 with two rocks and one gangue in the vertical direction and unloading direction is obvious, and the longitudinal fractures are developed. The fracture plane generated during the failure is parallel to the direction of the minimum horizontal principal stress, and the fracture is in the x-shaped conjugate shear failure mode.

Under the loading condition of plan 2, specimen C5 and two coals and one gangue B2, all specimens were damaged after unloading, while specimen A3 showed no obvious damage. The fracture plane orientation generated by specimen C5 with two rocks and one gangue is mostly parallel to the nonunloading direction, and the number of cracks in the specimens and the failure degree of the specimens are obviously smaller than those of specimen C6. The fracture plane orientation generated after loading of specimen B2 was mostly parallel to the nonunloading direction, and the number of cracks in the specimens and the failure degree of the specimens were significantly smaller than those of specimen B4.

Under the loading condition of plan 3, specimen C4 and specimen B6, no obvious failure occurred in all specimens after unloading, but obvious failure occurred in one rock and one coal A6. The rupture surface of specimen A6 is perpendicular to the unloading direction.

The interbedded specimens of coal-gangue undergo the process of initial fracture compression, microfracture development, mutual connectivity, and finally the formation of penetrating macro fracture. The failure mode is mainly pull-shear composite failure, and the macrofracture is obvious after the failure. The interbedded specimens of one rock and one coal show incomplete X-type conjugate shear failure characteristics. The coal specimens and rock specimens in the interbedded specimens of two coals and one gangue exhibit relatively independent and incomplete X-type conjugate shear failure characteristics, and transverse cracks are formed on the top of the coal specimens due to compression. The two-rock one-coal interbedded specimens exhibit systematic and incomplete *X*-type conjugate shear failure characteristics.

In the loading and unloading experiment of true triaxial simulation of real mining stress, the failure degree of samples with different gangue inclusion ratio is different under different loading conditions, statistics of the distribution of fragmentation after sample failure are shown in Figure 5, one coal one rock and two coal one rock samples have less damage after loading and unloading, the integrity of the sample is high, and the block cracks are concentrated in 12~15 cm. In the sample of one coal and two rocks, 60% of the failure lumpiness is concentrated in 12~15 cm, mainly in rock, and the failure lumpiness of coal is concentrated in 3~9 cm.

The size effect of coal-gangue mass after loading and unloading test is the reflection of its inherent structural complexity, which is due to the existence of fracture network system in rock mass and the joint influence of loading and unloading process. Coal-gangue physical and mechanical properties and particle distribution, as well as defects, such as joint distribution, showed a greater difference, the stress distribution of local stress and strain in different position is different, there will always be in the rock a very obvious damage crack, and this is the main cause of rock damage condition, thus, to some extent, limiting the development of

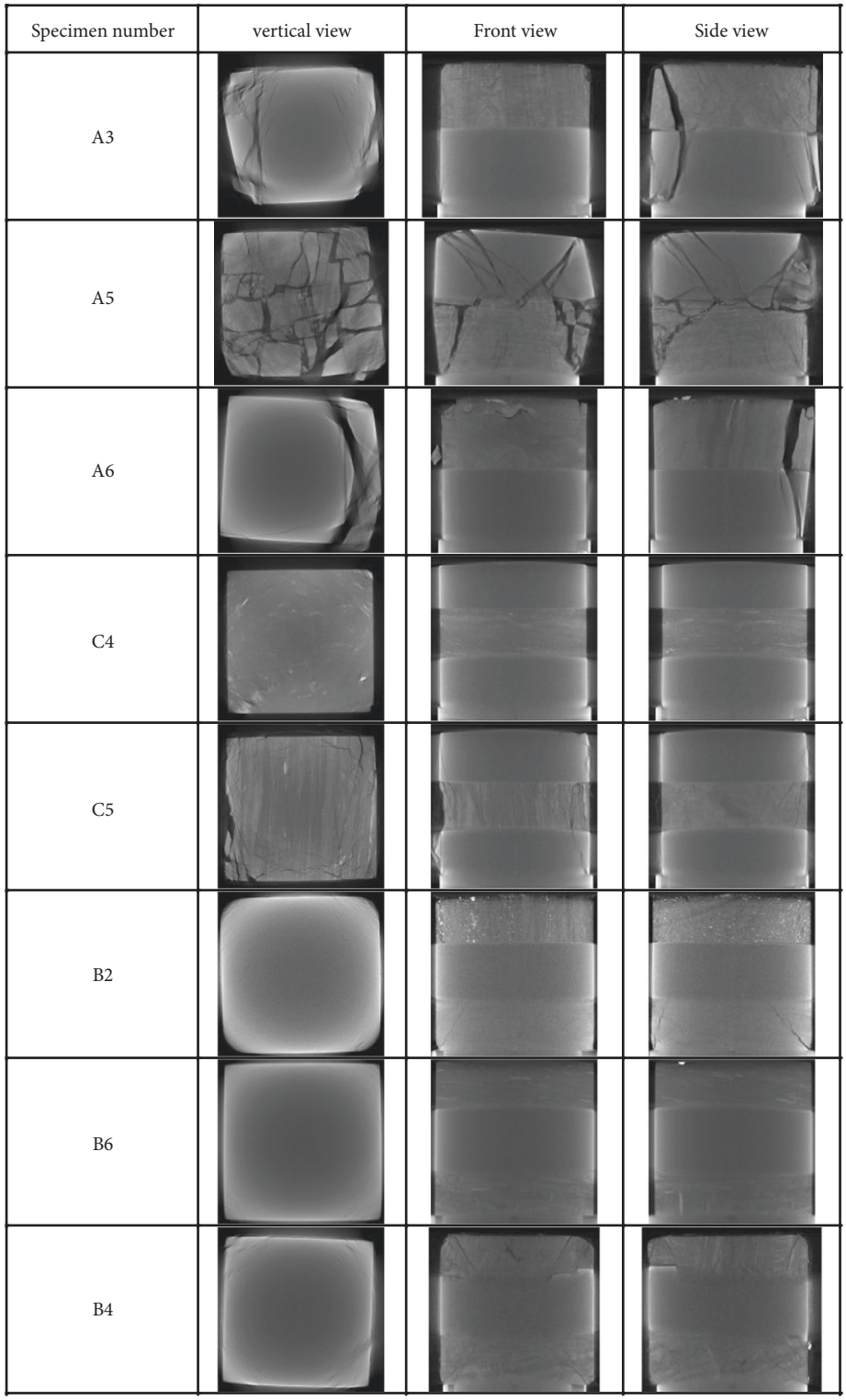

Figure 4: Micro-CT scanning results of coal-rock interbedding specimen after loading and unloading.

some of the other weak small cracks. The fragmentation resulting in damage is large.

3.2. Deformation Characteristics of Coal-Gangue Interbed Specimens with Different Ratios of Gangue. Loading and unloading tests were carried out under three axial pressures for each ratio of gangue. Figure 6 shows the body stress-strain curves of different ratio of gangue under different loading plans.

The specific results are as follows.

Under the vertical stress of 70 MPa, the stress-strain curve under each ratio of gangue shows the following: when

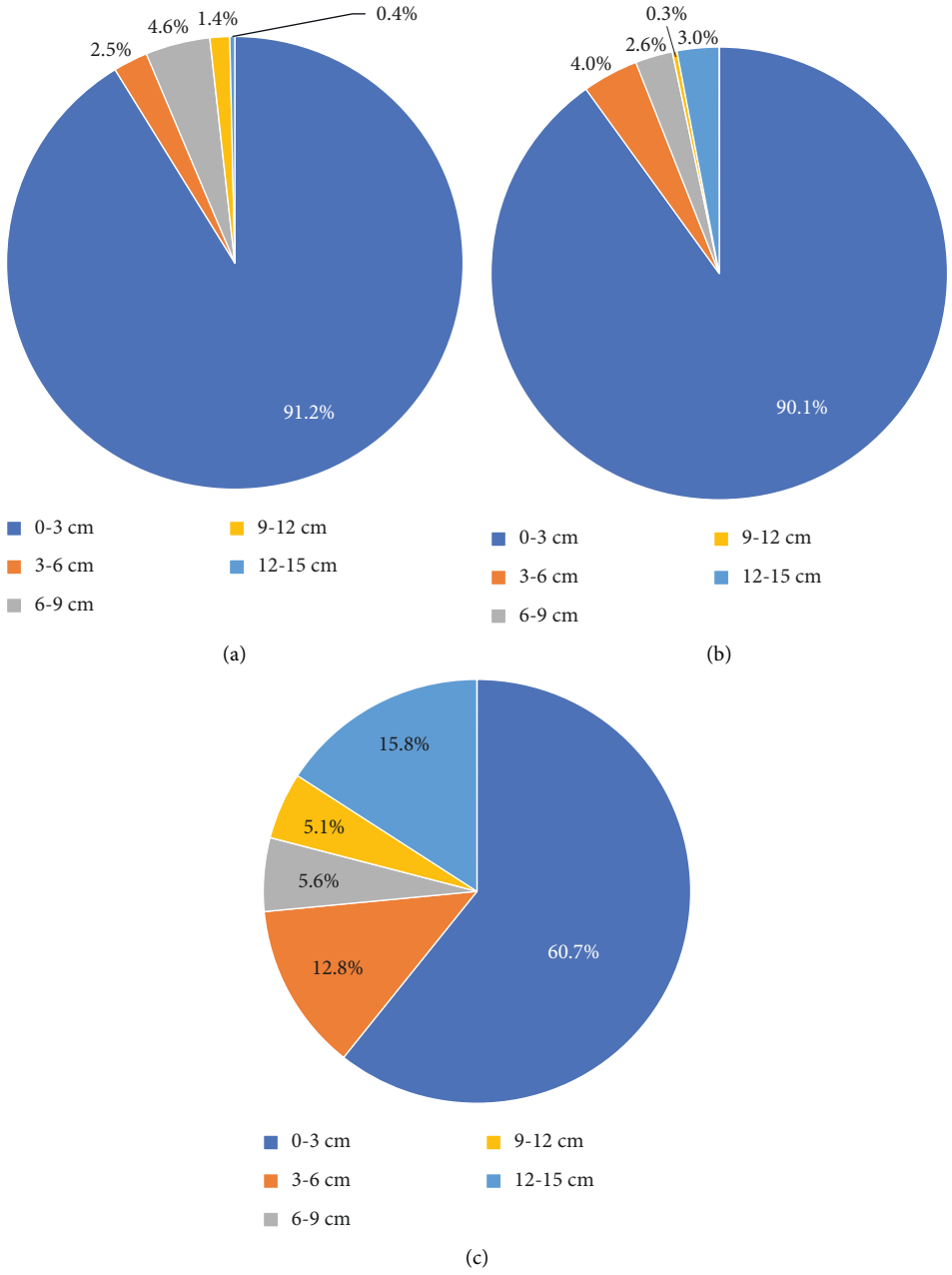

Figure 5: The block scale proportional distribution of different specimens. (a) One coal and one rock; (b) two coals and one rock; (c) one coal and two rocks.

the volume stress is low, one rock and one coal exhibit dilatation, while the other two groups of specimens do not exhibit dilatation, and the volume strain fluctuates or rises step by step with the increase of the volume stress. After that, the volume strain increases with the increase of volume stress, and the volume strain decreases with the increase rate of volume stress at 33.63 MPa. It can be found from the loading curve that when the volume stress reaches 33.63 MPa, the increase of volume stress is caused by the increase of spindle stress. When the bulk stress reaches 92 MPa, the bulk stress begins to decrease. Due to the difference of the loading and unloading paths and the new plastic deformation in the unloading process, the bulk strain decreases faster in the unloading stage than in the loading stage. The specimens with two rocks and one gangue, one rock and one coal, and two coals and one gangue failed at 77.79 MPa, 78.19 MPa, and 79.29 MPa, respectively, and the corresponding partial stresses were 70.42 MPa, 71.62 MPa, and 69.42 MPa, respectively. By comparing the volumetric stress-strain curves of specimens with different ratios of gangue at 33.63 MPa–92 MPa, it can be found that the increase rate of volumetric strain in this section decreases with the increase of the ratio of gangue.

Under the vertical stress of 60 MPa, the stress-strain curves under the conditions of various gangue ratios show the following: when the bulk stress is low, dilatancy occurs in

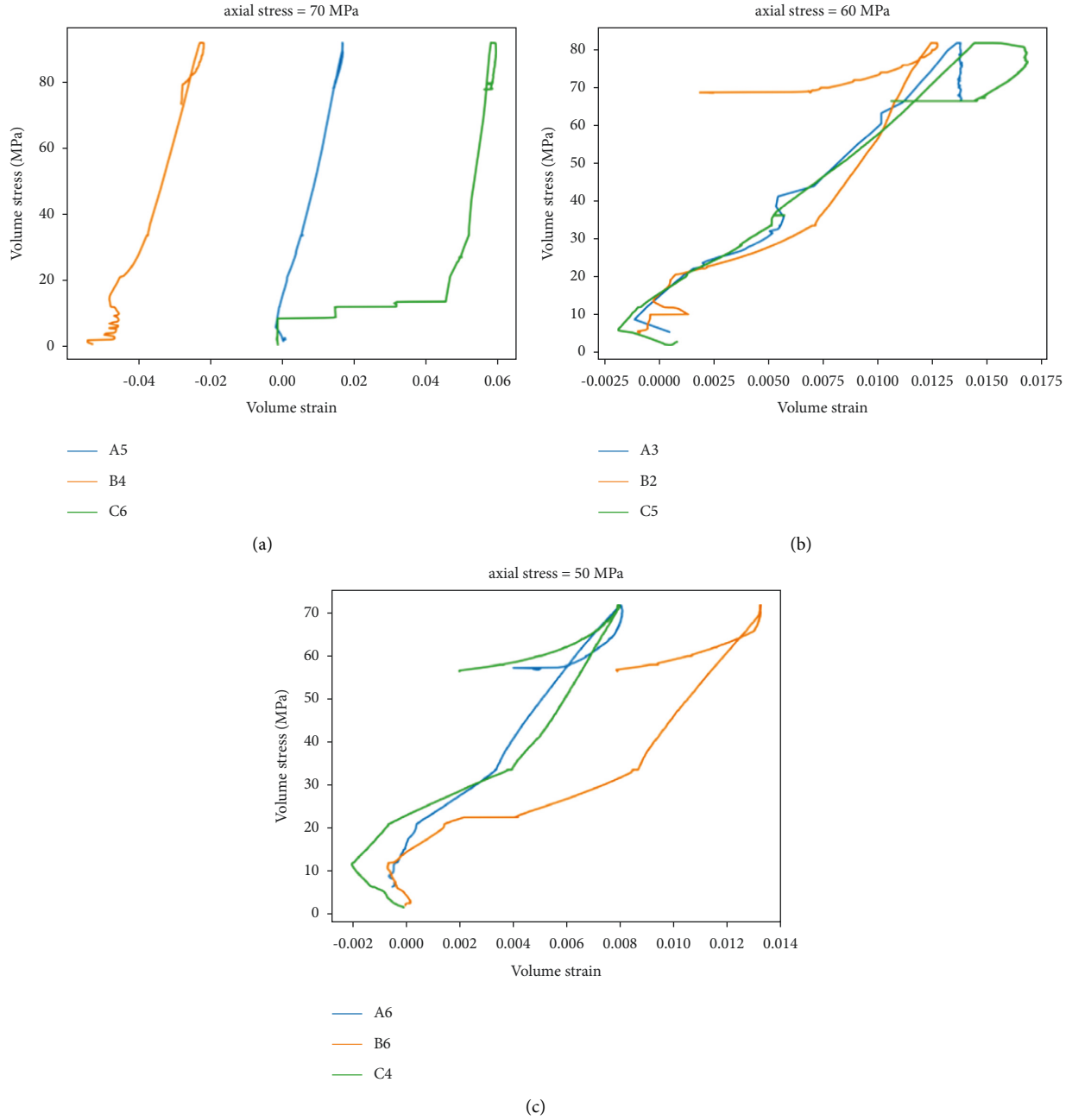

Figure 6: Volume stress-strain curve under different maximum vertical stress. (a) Maximum vertical stress = 70 MPa; (b) maximum vertical stress = 60 MPa; (c) maximum vertical stress = 50 MPa.

the specimens with one rock and one coal and two rocks and one gangue. The dilatancy does not occur in the specimens with two coals and one gangue. Around 20 MPa, the expansion volume offsets the previous dilatancy volume strain. After that, the bulk strain increases with the increase of bulk stress, and the bulk strain decreases with the increase rate of bulk stress at 35 MPa. From the loading curve, it can be found that the main shaft stress increases when the bulk stress reaches 35 MPa, and the stress-strain curves of one rock and one coal and two rocks and one gangue between 35 and 82 MPa are basically the same. When the bulk stress reaches 82 MPa, the bulk stress begins to decrease. Due to the difference of the loading and unloading paths and the new plastic deformation in the unloading process, the bulk strain decreases faster in the unloading stage than in the loading stage. By comparing the volumetric stress-strain curves of specimens with different ratios of gangue between 35 MPa and 82 MPa, it can be found that the volumetric strain rising rate decreases with the increase of the ratio of gangue. The specimens with two rocks and one gangue, one rock and one coal, and two coals and one gangue failed at 66.45 MPa, 66.45 MPa, and 68.94 MPa, respectively, and the corresponding partial stresses were 65.1 MPa, 65.1 MPa, and 60.12 MPa, respectively.

Under the vertical stress of 50 MPa, the stress-strain curve under the conditions of each gangue ratio shows the following: when the volume stress is low, dilatation phenomenon occurs in the specimens of one coal and one coal as well as two coals and onecoal. No dilatation occurs in the specimens of two coals and one rock. After that, the volume strain increases with the volume stress increasing, and the volume strain decreases with the growth rate of the volume stress at 34 MPa. From the loading curve, it can be found that when the volume stress reaches 34 MPa, the increase of the volume stress is caused by the increase of the principal axis stress. The volume strain increment of the three specimens is basically the same between 34 and 72 MPa. When the bulk stress reaches 72 MPa, the bulk stress begins to decrease. Due to the difference of the loading and unloading paths and the possible new plastic deformation during the unloading process, the bulk strain decreases faster in the unloading stage than in the loading stage. After loading and unloading, the specimens with one rock and one coal and two coals and one gangue were destroyed at 57.32 MPa and 56.67 MPa, respectively, and the corresponding partial stress was 53.36 MPa and 54.66 MPa, respectively.

Based on the test results of the three groups of loading conditions, the influence of different gangue ratio on the mechanical properties of coal-gangue interbed specimens can be obtained. The influence of gangue ratio on the structural strength of coal-gangue interbed is significant, mainly reflected in the two following aspects: (a) With the decrease of the ratio of gangue, the deformation in the direction of the maximum principal stress increases, while the deformation in the unloading direction does not change significantly. The corresponding volume strain increases, indicating that the deformation required before specimen failure increases. (b) As the ratio of gangue increases, the critical volume stress for failure of coal-gangue interbedded structure rises, indicating that the higher the ratio of gangue in unloading process, the stronger the stability of coal-gangue interbedded structure.

3.3. Changes in Bulk Modulus of Specimens with Different Ratios of Gangue. The bulk modulus between the body stress of 20 MPa and the maximum principal stress during loading and unloading was calculated, as shown in Table 2.

As the ratio of gangue increases, the bulk modulus of coal-gangue interbedded sample decreases. The correlation between the ratio of gangue and the bulk modulus is drawn, as shown in Figure 7. The relationship between the ratio of gangue and the bulk modulus of coal-gangue interbedded sample is quadratic polynomial.

Table 2: The bulk modulus of specimen with different gangue ratio.

Specimens number	The type of specimens	Bulk modulus (Pa)
A3	One rock and one coal	4909.339
A5	One rock and one coal	6181.396
A6	One rock and one coal	6796.158
	Average value	**5962.298**
B2	One rock and two coals	5083.113
B4	One rock and two coals	4534.259
B6	One rock and two coals	4236.436
	Average value	**4617.936**
C4	Two rocks and one coal	4812.791
C5	Two rocks and one coal	4659.832
C6	Two rocks and one coal	3169.501
	Average value	**4214.041**

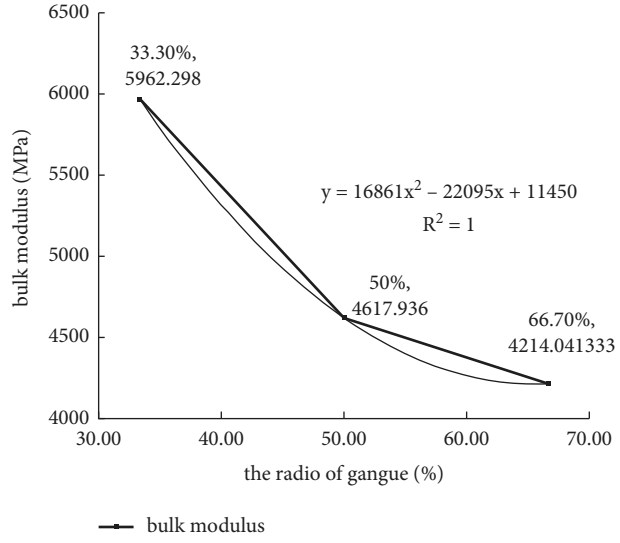

Figure 7: The relationship between gangue ratio and bulk modulus.

4. Numerical Simulation Analysis of Fracture Characteristics of Coal-Rock Interbedding

4.1. Numerical Modeling and Simulation Solutions. Generally, the computational domains include the continuous state, discontinuous state, or partially continuous state, which correspond to the FEM, DEM, and CDEM domains. Conventionally, the FEM domain is used for fully continuous problems, and the DEM domain for fully discontinuous problems. Meanwhile the Continuous Discontinuous Element Method (CDEM) couples the finite element calculation with the discrete element calculation, which conducts finite element calculation inside the block elements and conducts discrete element calculation at the block elements boundary. Through the fracture of interface elements, not only can the deformation and motion characteristics of the material in the continuous state and the discontinuous state be simulated, but also the progressive failure process of the material from the continuous body to the discontinuous body can be realized. In this paper, considering the influence of coal seam gangue, the high-efficiency numerical simulation software GDEM based on CDEM theory is used to conduct numerical simulation research on the failure process of coal-rock interbedded specimens under triaxial loading.

To study the influence law of coal and gangue on the mixed-bed specimen failure, based on the specimen types of laboratory tests, the numerical models of one-coal two-rock specimen, one-coal one-rock specimen, and two-coal one-

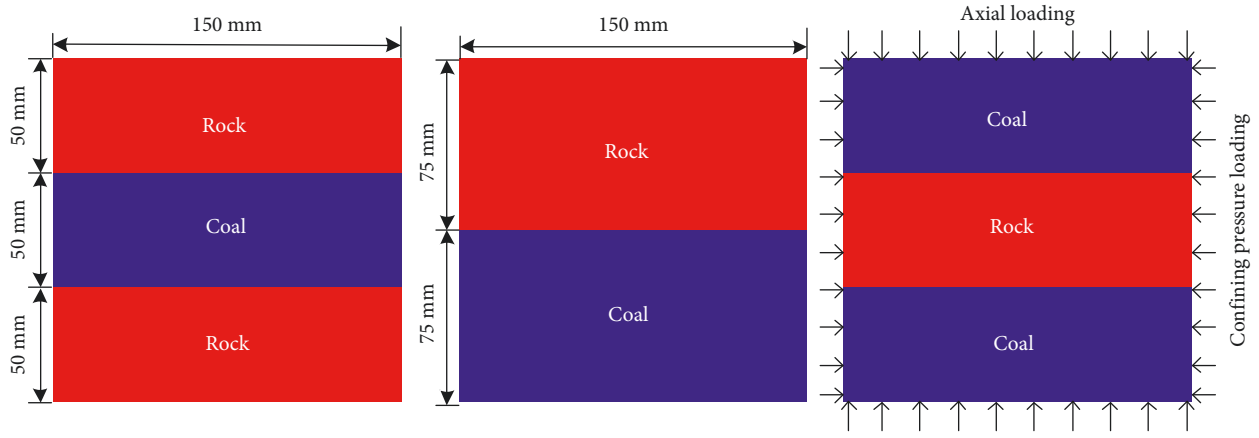

Figure 8: Numerical models and boundary conditions.

Table 3: Micromechanical parameters of coal-rock sample.

	Density (kg/m^3)	Elastic modulus (Pa)	Poisson's ratio	Cohesion (MPa)	Tensile strength (MPa)	Internal friction angle (°)
Rock	2500	8.51e9	0.26	20.2	27.04	30.0
Coal	1300	2.69e9	0.34	14.6	19.68	26.0

rock specimen are generated. The element number of numerical model is 22500, and the width of numerical model is 150 mm. For one-coal two-rock specimen and two-coal one-rock specimen, the heights of rock layer and coal layer in numerical model are 50 mm. For one-coal one-rock specimen, the heights of rock layer and coal layer are 75 mm. To simulate the triaxial loading of rock test, the vertical compressive stress is applied to the upper and lower surfaces of numerical model to simulate the axial loading, and the horizontal compressive stress is applied to the left and right surfaces of numerical model to simulate the confining pressure loading. The size of the model size and boundary conditions numerical specimen is 150 mm × 150 mm, as shown in Figure 8.

According to the mechanical test results of the rock specimen, the mesomechanical parameters of the coal-rock specimen in the simulation are obtained through numerical inversion, as shown in Table 3.

A large number of research works indicate that the maximum principal stress in the vertical bedding direction is the main factor causing the coal-gangue interbedding. Therefore, based on the experimental scheme of coal-rock specimens, three axial pressures of 50 MPa, 60 MPa, and 70 MPa are, respectively, used in the numerical simulation, and the maximum horizontal principal stress is 12 MPa. The simulations of loading and unloading process of coal-rock specimens under three combination conditions are carried out. During the simulation, uniformly distributed compressive stresses of 50 MPa, 60 MPa, and 70 MPa are, respectively, applied to the upper and lower surfaces of the coal-rock specimen, and the uniformly distributed horizontal compressive stress of 12 MPa is applied to the left and right surfaces of the coal-rock specimen. During the loading process, when the simulation iterates for 100,000 steps, the loading process ends, and the damage and failure degree of the coal-rock specimen is analyzed. To simulate the failure mechanism of the coal-rock structure under the asymmetric load of mining disturbance during the coal mining process, the simulation scheme of unloading the confining pressure on one side of the specimen is adopted to study the failure mechanism of the coal-rock sample.

4.2. Specimen Failure Characteristics during Unloading. Under the axial pressure of 50 MPa, 60 MPa, and 70 MPa and confining pressure of 12 MPa, after unloading the confining pressure on the right side of the specimen, the failure results of the coal-rock specimen under different combination conditions are shown in Figure 9.

From Figure 9, for one rock-one coal specimen, under the axial pressure of 50 MPa, the confining pressure of 12 MPa is unloaded, the length of the crack from the unloading boundary to the middle of the specimen gradually shortens, and the length of the crack in the coal seam is smaller than that of the rock layer; however, there are obvious fracture zones in the coal seam. With the increase of the loading axial pressure, the coal-rock specimen presents a tendency to fly outwards after unloading the confining pressure, and the tendency of the coal seam to fly away is more obvious. With the increase of the loading axial pressure, the width of the oblique fracture zone in the coal seam increases significantly after the confining pressure. For the one-rock two-coal specimen, with the increase of the loading axial pressure, the distribution range of the cracks in the specimen increases after unloading the confining pressure. The upper and lower coal seams of the specimen are thrown out symmetrically after unloading the confining pressure; however, there is no obvious tendency of being thrown away in the middle rock layer, and the specimen as a whole showed a concave failure shape. For the two-rock one-

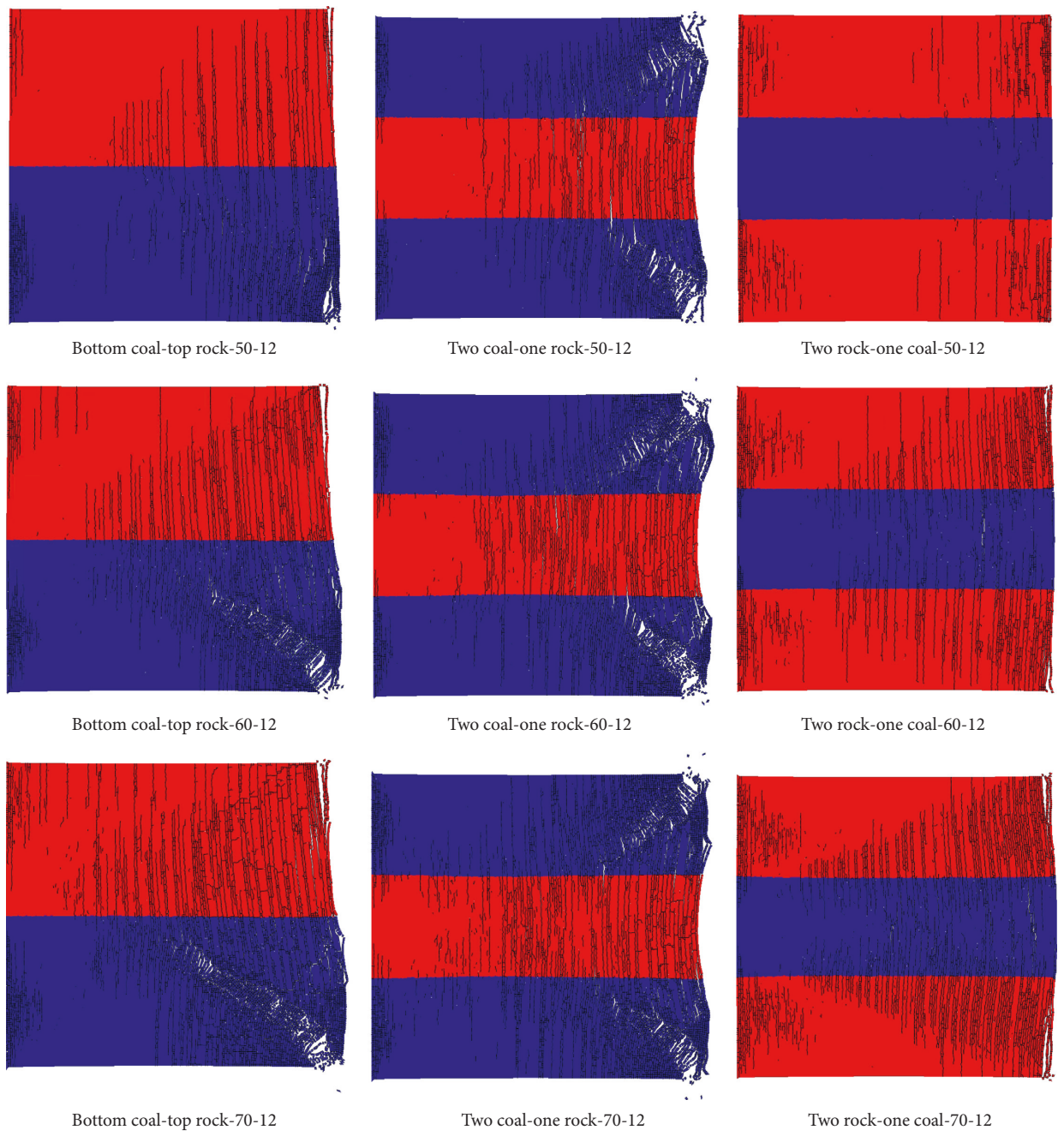

Figure 9: Failure results of rock sample after unloading the confining pressure. (a) Bottom coal-top rock, 50-12; (b) top coal-one rock, 50-12; (c) two rocks-one coal, 50-12; (d) bottom coal-top rock, 60-12; (e) top coal-one rock, 60-12; (f) two rocks-one coal, 60-12; (g) bottom coal-top rock, 70-12; (h) top coal-one rock, 70-12; (i) two rocks-one coal, 70-12.

coal specimen, under the axial pressure of 50 MPa, the upper and lower rock layers of the specimen are obviously fractured after unloading confining pressure, and the damage degree of the middle coal seam is weaker. Under the axial pressure of 60 MPa and 70 MPa, the cracks in coal and rock layers of sample are obvious after unloading. Under different loading and unloading conditions, the two-rock one-coal specimens show a convex failure form in which the central coal seam protrudes outwards. As a whole, the greater the loading axial pressure, the greater the damage degree of different coal-rock specimens after unloading; different specimens all produce significant unloading-tensile failure on the side of the unloading boundary; the failure degree of the two-coal one-rock specimen is greater than that of the one-coal one-rock specimen which is greater than that of the one-coal two-rock specimen.

5. Conclusions

(1) The influence of the proportion of coal-rock interbed structure is significant, mainly embodied in the two following aspects; first, with the proportion of dirt

band down the direction of maximum principal stress deformation on the rise, change of the direction of the unloading deformation is not obvious, the corresponding volume strain increases, the characterization of the specimen to before the damage deformation increases; second, as the ratio of gangue decreases, the critical volume stress of coal-gangue interbedded structure increases, indicating that the higher the ratio of gangue in unloading process, the stronger the stability of coal-gangue interbedded structure.

(2) Under the condition that the maximum horizontal principal stress value is determined, with the unloading process, different degrees of asynchronous damage and failure will occur in the coal-gangue interbedded layer of top coal body. In the vertical direction, the coal-gangue interbedded layer of top coal body presents various types of failure characteristics according to the change of horizontal stress gradient.

(3) The interbedded specimens of coal-gangue undergo a process of initial fracture compression, microfracture development, mutual connectivity, and finally the formation of penetrating macrofractures. The failure mode is mainly pulse-shear composite failure, and the macrofractures are obvious after the failure. When the maximum horizontal principal stress is greater than 60 MPa, the specimen after unloading is relatively broken, and the size of block cracks is concentrated in 12–15 cm. With the increase of the ratio of gangue, the incomplete X-type conjugate shear failure is more obvious.

(4) During the triaxial loading process, the coal-gangue interlayer specimens with different combinations generate the microfractures near the confining pressure loading boundary. After unloading confining pressure, different specimens all generate obvious tensile failure on the side of the unloading boundary. The greater the loading axial pressure, the greater the damage degree of the specimen after unloading. The damage degree of the two-coal one-rock specimen is greater than that of the one-coal one-rock specimen which is greater than that of the one-coal two-rock specimen.

Data Availability

The data used to support the findings of this study are available from the corresponding author upon request.

Conflicts of Interest

The authors declare that there are no conflicts of interest regarding the publication of this paper.

Acknowledgments

This work was supported by the National Key Research and Development Program (2018YFC0604506) and Science and Technology Innovation and Entrepreneurship Fund Special Project of Tiandi Technology Co., Ltd. (2020-TD-ZD016).

References

[1] Y. Luo, *Research on Evolution of Roof Force Chain and Top Coal Failure Law in Fully Mechanized Caving Stope*, Master Thesis of Anhui University of Science and Technology, Anhui, China, degree programs, 2016.

[2] J. C. Wang and Z. H. Wang, "The failure mechanism of top coal in fully mechanized caving mining under the combined action of loading and unloading," *Tongmei Science and Technology*, vol. 155, no. 3, p. 1~7, 2017.

[3] J. P. Zuo, J. L. Pei, J. F. Liu, and R. D. Peng, "Acoustic emission behavior and space-time evolution mechanism in the process of coal and rock fracture," *Chinese Journal of Rock Mechanics and Engineering*, vol. 30, no. 8, pp. 1564–1570, 2011.

[4] B. X. Liu, J. L. Huang, Z. Y. Wang, and L. Liu, "Study on damage evolution and acoustic emission characteristics of uniaxial compression coal and rock," *Chinese Journal of Rock Mechanics and Engineering*, vol. 28, no. S1, pp. 3234–3238, 2009.

[5] E. Y. Wang and X. Q. He, "Experimental study on electromagnetic radiation of coal and rock deformation and fracture," *Chinese Journal of Geophysics*, no. 1, pp. 131–137, 2000.

[6] X. R. Ge, J. X. Ren, and Y. B. Pu, "CT dynamic test of triaxial mesoscopic damage evolution law of coal and rock," *Chinese Journal of Rock Mechanics and Engineering*, no. 5, pp. 497–502, 1999.

[7] B. Bai, N. Qingke, Z. Yike, W. Xiaolong, and H. Wei, "Co-transport of heavy metals and SiO 2 particles at different temperatures by seepage," *Journal of Hydrology*, vol. 597, 2020.

[8] B. Yuan, Z. Li, W. Chen et al., "Influence of groundwater depth on pile-soil mechanical properties and fractal characteristics under cyclic loading," *Fractal and Fractional*, vol. 6, no. 4, p. 198, 2022.

[9] Y. D. Jiang, Y. S. Pan, and F. X. Jiang, "Mechanism and prevention of rock burst in coal mining in my country," *Journal of Coal Science*, vol. 39, no. 2, pp. 205–213, 2014.

[10] Y. J. Yang, Y. Song, and J. Chu, "Experimental study on strength and deformation characteristics of coal and rock under cyclic loading," *Chinese Journal of Rock Mechanics and Engineering*, no. 1, pp. 201–205, 2007.

[11] Y. X. Xia, J. F. Pan, and Y. J. Wang, "Research on coal rock fracture and stress distribution characteristics based on high-precision microseismic monitoring," *Journal of Coal Science*, vol. 36, no. 2, pp. 239–243, 2011.

[12] B. Yuan, L. Zihao, C. Yiming et al., "Mechanical and microstructural properties of recycling granite residual soil reinforced with glass fiber and liquid-modified polyvinyl alcohol polymer," *Chemosphere*, vol. 286, 2021.

[13] B. Yuan, Z. Li, and Z. Zhao, "Experimental study of displacement field of layered soils surrounding laterally loaded pile based on transparent soil," *Journal of Soils and Sediments*, vol. 4, pp. 1–12, 2021.

[14] B. Bai, R. Zhou, G. Cai, W. Hu, and G. Yang, "Coupled thermo-hydro-mechanical mechanism in view of the soil particle rearrangement of granular thermodynamics," *Computers and Geotechnics*, vol. 137, Article ID 104272, 2021.

[15] P. S. Xie, Y. Y. Zhang, and Y. L. Zhang, "Instability law of interlayer roof in large dip angle and high mining height and its influence on support," *Chinese Journal of Coal*, vol. 46, no. 2, pp. 344–356, 2021.

[16] C. J. Zhu, C. Ma, and J. X. Zhou, "Mechanical properties and failure characteristics of composite coal-rock mass under the coupling of dynamic and static loads," *Journal of Coal*, vol. 38, 2021.

[17] Y. P. Wu, W. H. Liu, Y. L. Zhang, and W. B. Yang, "Deformation and failure characteristics of overlying rock in coal-rock interbedded roof with large dip angle and large mining height," *Mining Research and Development*, vol. 40, no. 9, p. 5, 2020.

[18] Z. T. Zhang, J. F. Liu, L. Wang, and M. Zhao, "Experimental study on the influence of combination method on the mechanical properties and failure characteristics of coal-rock combination," *Chinese Journal of Coal*, vol. 37, no. 10, pp. 1677–1681, 2012.

[19] B. S. Nie, X. Q. He, and C. W. Zhu, "Study on mechanical properties and electromagnetic emission during the fracture process of combined coal-rock," *Procedia Earth and Planetary Science*, vol. 1, no. 1, pp. 281–287, 2009.

[20] Z. H. Zhao, W. M. Wang, L. H. Wang, and C. Dai, "Compression-shear strength criterion of coal-rock combination model considering interface effect," *Tunnelling and Underground Space Technology*, vol. 47, pp. 193–199, 2015.

[21] S. K. Zhao, Y. Zhang, and R. J. Han, "Numerical simulation of impact tendency evolution of combined coal-rock structure," *Journal of Liaoning University of Engineering and Technology (Natural Science Edition)*, vol. 32, no. 11, pp. 1441–1446, 2013.

[22] Z. H. Chen, C. A. Tang, and R. Q. Huang, "A double rock sample model for rockbursts," *International Journal of Rock Mechanics and Mining Sciences*, vol. 34, no. 6, pp. 991–1000, 1997.

[23] B. X. Huang and J. W. Liu, "The effect of loading rate on the behavior of samples composed of coal and rock," *International Journal of Rock Mechanics and Mining Sciences*, vol. 61, pp. 23–30, 2013.

[24] J. X. Liu, C. A. Tang, and W. C. Zhu, "Study on coal-rock series combination model and rock burst mechanism," *Chinese Journal of Geotechnical Engineering*, vol. 26, no. 2, pp. 276–280, 2004.

[25] C. P. Lu, L. M. Dou, and X. R. Wu, "Experimental study on the evolution of the impact tendency and the acousto-electric effect of the combined coal and rock," *Chinese Journal of Rock Mechanics and Engineering*, vol. 26, no. 12, pp. 2549–2555, 2007.

[26] L. M. Dou, J. C. Tian, and C. P. Lu, "Study on electromagnetic radiation law of combined coal and rock impact damage," *Chinese Journal of Rock Mechanics and Engineering*, vol. 24, no. 19, pp. 3541–3544, 2005.

[27] H. P. Xie, Z. H. Chen, and H. W. Zhou, "A preliminary study on the two-body mechanical model based on the interaction between engineering body and geological body," *Chinese Journal of Rock Mechanics and Engineering*, vol. 24, no. 9, pp. 1457–1464, 2005.

[28] J. P. Zuo, H. P. Xie, and A. M. Wu, "Study on the failure mechanism and mechanical properties of deep coal-rock individual and assemblage," *Chinese Journal of Rock Mechanics and Engineering*, vol. 30, no. 1, pp. 84–92, 2011.